TGF-β–Mediated Modulation of Cell–Cell Interactions in Postconfluent Maturing Corneal Endothelial Cells

Kim Santerre,[1–3] Sergio Cortez Ghio,[1,2] and Stéphanie Proulx[1–3]

[1]Centre de recherche du Centre hospitalier universitaire (CHU) de Québec–Université Laval, axe médecine régénératrice, Hôpital du Saint-Sacrement, Québec, Québec, Canada
[2]Centre de recherche en organogénèse expérimentale de l'Université Laval/LOEX, Québec, Québec, Canada
[3]Département d'Ophtalmologie et d'oto-rhino-laryngologie-chirurgie cervico-faciale, Faculté de médecine, Université Laval, Québec, Québec, Canada

Correspondence: Stéphanie Proulx, Centre de recherche du CHU de Québec–Université Laval, site de l'Hôpital du Saint-Sacrement, 1050 Chemin Sainte-Foy, Québec, QC G1S 4L8, Canada; stephanie.proulx@fmed.ulaval.ca.

Received: March 25, 2022
Accepted: August 6, 2022
Published: October 4, 2022

Citation: Santerre K, Cortez Ghio S, Proulx S. TGF-β–mediated modulation of cell–cell interactions in postconfluent maturing corneal endothelial cells. *Invest Ophthalmol Vis Sci.* 2022;63(11):3. https://doi.org/10.1167/iovs.63.11.3

Purpose. Transforming growth factor-beta (TGF-β) is known to influence many cell functions. In the corneal endothelium, TGF-β1 exerts contextual effects, promoting endothelial–mesenchymal transition in proliferating cells and enhancing barrier integrity in early confluent maturing cells. Herein, we studied how TGF-β isoforms participate in the formation of corneal endothelial intercellular junctions.

Methods. Corneal endothelial cells (CECs) were cultured using a two-phase media approach. When CECs reached confluence, the proliferation medium was replaced with maturation medium, which was supplemented or not with TGF-β isoforms. The cell morphology (circularity index), intercellular junction protein expression, transendothelial electrical resistance (TEER), and permeability of 7-day postconfluent CECs were assessed. Gene transcription and signaling pathways that were activated following maturation in the presence of TGF-β2 were also studied. The beneficial effect of TGF-β2 on CEC maturation was evaluated using ex vivo corneas mounted on a corneal bioreactor.

Results. The results showed increases in circularity index, membrane localization of junction-related proteins, and TEER when TGF-β isoforms were individually added during the maturation phase, and TGF-β2 was the most effective isoform. Gene profiling revealed an increase in extracellular matrix-related gene expression. In ex vivo cell adhesion experiments, CECs that were matured in the presence of TGF-β2 had a higher circularity index and cell density and exhibited cell membrane-localized junction-related protein expression at earlier time points.

Conclusions. These results suggest that TGF-β2 can strengthen cell–cell and cell–substrate adhesion, which accelerates barrier integrity establishment and thus enhances CEC functionality.

Keywords: corneal endothelial cells, TGF-β, intercellular junctions, extracellular matrix

The corneal endothelium is a thin monolayer of hexagonal cells that forms a leaky barrier between the aqueous humor of the anterior chamber and the corneal stroma. Adherens and tight junctions, located on the lateral membranes of corneal endothelial cells (CECs),[1] are responsible for cell–cell adhesion and occlude the paracellular space to inhibit the fluid leak generated by the swelling pressure associated with the hydrophilic glycoaminoglycans of the corneal stroma.[2] This fluid leak is counterbalanced by an active pump mechanism that drives fluid from the stroma back into the anterior chamber, preventing corneal edema.[2] A breach in intercellular junctions results in an increase in aqueous humor leakage into the corneal stroma, altering the "pump–leak" balance and causing vision loss.[3]

Human CEC density is approximately 6000 cells/mm^2 at birth[4] and decreases throughout life at an average rate of 0.6% per year,[5] reaching 2300 cells/mm^2 at age 85.[6] When a cell dies, neighboring cells need to fill the gap to reform a functional barrier, and they do so via cell migration and cell spreading; this phenomenon partially explains the decrease in endothelial cell density and the increase in polymegethism and pleomorphism. Therefore, throughout life, CECs transiently need to quickly reform intercellular junctions to avoid an increased influx of aqueous humor into the stroma.

It is possible to study intercellular junction formation using cultured CECs. After cultured CECs reach confluence, they progressively adopt a mature phenotype of hexagonal cells. This process requires many weeks of culture at postconfluent stages. For example, a gradual maturation of N-cadherin was reported in human cultured CECs, reaching a pattern similar to that observed in vivo after 21 days of culture.[7] When optimizing markers of functional CECs for cell therapy, the Kinoshita group[8] developed a method to quantify the number of "effector" cells (authors defined "effector cells" as the side population of CECs that would be applicable for cell therapy) in culture using an "E-ratio" (CD166+/CD44–/CD105–/CD26–/CD24–/CD133–). These authors showed that this ratio gradually increased

Table. Tissue Donor Details

Donor	Age (y)	Sex	Cause of Death	Use
1	75	M	Unavailable	Circularity, immunofluorescence, TEER
2	62	M	Infarctus	Circularity, immunofluorescence, TEER
3	70	M	Pulmonary neoplasia	Circularity, immunofluorescence, TEER
4	84	M	Colon neoplasia	Circularity, immunofluorescence, TEER
5	57	F	Infarctus	TEER, permeability
6	55	M	Kidney neoplasia	TEER, permeability
7	67	F	Cerebral hemorrhage	TEER, permeability
8	68	F	Pulmonary neoplasia	Ca^{2+}-switch assay
9	60	F	Infarctus	Ca^{2+}-switch assay
10	45	F	Cerebral hemorrhage	Ca^{2+}-switch assay
11	45	F	Metastatic breast neoplasia	Gene profiling, TGF-β array
12	55	M	Unavailable	Gene profiling, TGF-β array
13	59	F	Unavailable	Gene profiling
14	72	M	Pulmonary neoplasia	Gene profiling, TGF-β array
15	50	M	Pulmonary neoplasia	Devitalized
16	58	M	Pulmonary neoplasia	Devitalized
17	66	M	Coma	Devitalized
18	52	F	Metastatic breast neoplasia	Devitalized
19	60	F	Pulmonary neoplasia	Devitalized
20	79	F	Pulmonary neoplasia	Adhesion assay
21	60	M	Stomach neoplasia	Adhesion assay
22	71	M	Respiratory failure	Adhesion assay
23	68	M	Pulmonary neoplasia	Adhesion assay

from week 1 to week 3 of cell culture, further demonstrating the beneficial effect of prolonged culture times for the maturation of CECs.

We previously demonstrated that transforming growth factor-beta 1 (TGF-β1) exerted contextual effects on CECs.[9] Although TGF-β1 induced a fibroblastic-like morphology in subconfluent CECs (proliferative phase), it restored a polygonal cell shape and cell–cell junctions in 7-day postconfluent cells (maturation phase).[9] Compared to controls, TGF-β1 allowed the quick reformation of a functional barrier in vitro. As aqueous humor contains all three isoforms of TGF-β (TGF-β2 being the most concentrated[10]), we hypothesized that TGF-β isoforms may function to help maintain the homeostasis of the corneal endothelium, especially regarding barrier integrity. We investigated whether all three TGF-β isoforms exerted effects on morphology, cell–cell junctions, and in vitro functionality. To study its influence on the formation of intercellular junctions, we performed gene expression and cell signaling analysis using CECs that were matured in the presence of TGF-β2. We also tested the beneficial effect of TGF-β2 maturation on cell adhesion by injecting cells into a bare Descemet's membrane using ex vivo corneas mounted on a corneal bioreactor.[11]

Methods

All of the experiments were conducted in accordance with the tenets of the Declaration of Helsinki. The research protocol was approved by the "Bureau de l'éthique de la recherche du CHU de Québec–Université Laval" ethics committee (DR-002-1382).

Cell Isolation and Culture

Pairs of research-grade corneas (n = 23) from cadavers were obtained from our local Eye Bank, Banque d'yeux du Centre universitaire d'ophtalmologie (CUO), CHU de Québec, Québec, QC, Canada. The donor age ranged from 45 to 84 years (62 ± 10 years) (Table). Research-grade corneas are those that were rejected for clinical use by the eye bank because of low endothelial cell density or expired delays in Optisol. The corneal endothelium and Descemet's membrane were peeled off, and the strips were incubated in collagenase A (1 mg/mL) for 3 to 4 hours before being seeded on dishes coated with FNC Coating Mix (AthenaES, Baltimore, MD, USA).[12]

At every subsequent passage, the nearly confluent CECs were dissociated with trypsin (0.05%)–EDTA (0.53 mM; Corning Inc., Corning, NY, USA), manually counted with a hemacytometer, and seeded at a density of 20,000 cells/cm^2, which corresponds to a 1:2 to 1:3 dilution, depending on the amount of cells.[12] At this initial cell density, cells take an average of 4 days before reaching near confluency. All of the experiments were conducted using passage 3 cells.

CECs were cultured following a previously described two-phase media approach.[9,12] During the proliferation phase, CECs were cultured in proliferation medium (P-medium) consisting of Opti-MEM I basal medium (Life Technologies, Carlsbad, CA, USA) supplemented with 8% fetal bovine serum (FBS; Life Technologies), 5 ng/mL epidermal growth factor (Austral Biologicals, San Ramon, CA, USA), 0.08% chondroitin sulfate (Sigma-Aldrich, St. Louis, MO, USA), 20 µg/mL ascorbic acid (Sigma-Aldrich), and streptavidin/penicillin (VWR, Radnor, PA, USA). When the CECs reached confluence, the proliferation medium was replaced with maturation medium (M-medium) consisting of Opti-MEM I medium (Life Technologies) supplemented with 8% FBS and streptavidin/penicillin (VWR). The M-medium was supplemented or not with 5 ng/mL recombinant human active TGF-β1, TGF-β2, or TGF-β3 (R&D Systems, Minneapolis, MN, USA), which was added at each medium change. The medium was changed every 2 to 3 days. CECs were maintained in M-medium for 7 days before analysis.

Investigative Ophthalmology & Visual Science

Circularity Index Analysis

The cell circularity index (CI) was calculated based on phase-contrast images taken at every medium change with a phase-contrast microscope (Nikon, Tokyo, Japan) and Zen acquisition software. The formula used to calculate the CI was CI = 4π(area/perimeter^2).[13] The area and perimeter were manually measured using ImageJ (National Institutes of Health, Bethesda, MD, USA). One hundred cells from four micrographs per condition per population were analyzed. Using this formula, a cell with a perfectly circular morphology would have a circularity index of 1, and an elongated cell would have a value closer to 0. As a reference, the native CEC CI was calculated from electronic microscopy images and had a value of 0.87 $\pm$ 0.03. Cell morphology was classified according to the average CI: endothelial/hexagonal morphology (CI $>$ 0.68), intermediate morphology (CI = 0.68–0.55), and fibroblastic-like/elongated morphology (CI $<$ 0.55).[14]

Indirect Immunofluorescence

Cells cultured on glass coverslips or on inserts as indicated were fixed with 4% paraformaldehyde for 20 minutes at room temperature and washed three times with phosphate-buffered saline (PBS). Next, the cells were permeabilized with 0.2% Thermo Scientific Triton X-100 (Thermo Fisher Scientific, Waltham, MA, USA) for 10 minutes before blocking with 5% bovine serum albumin (Sigma-Aldrich) diluted in PBS for 30 minutes. Primary antibodies—mouse monoclonal anti-N-cadherin (Agilent Technologies, Santa Clara, CA, USA), mouse monoclonal anti-ZO1 (Thermo Fisher Scientific), or mouse monoclonal anti-β-catenin (Agilent Technologies)—were added and incubated for 1 hour at room temperature. The cells were washed three times in PBS, and then the secondary antibody (anti-mouse IgG conjugated to Alexa Fluor 594; Thermo Fisher Scientific) and counterstains (Hoechst-33258; Sigma-Aldrich) were added and incubated for 1 hour at room temperature in the dark. Coverslips were mounted on glass slides with mounting media and stored at 4°C until observation. Micrographs were taken with a confocal microscope (ZEISS LSM 800; Carl Zeiss Meditec, Jena, Germany) and Zen acquisition software.

Trans-Endothelial Electrical Resistance Assay

CECs were seeded on standing culture inserts (EMD Millipore, Burlington, MA, USA) covered with FNC Coating Mix and cultured following the two-phase culture approach as described above. When the cells reached confluence, trans-endothelial electrical resistance (TEER) measurements were taken at every media change for a total of four time points. The medium was first changed, and TEER (Millicell ERS-2 Voltohmmeter; EMD Millipore) was measured after letting the fresh medium equilibrate for at least 30 minutes. During TEER measurements, CEC cultures were maintained at 37°C on a warming plate. The electrical resistance was normalized to the culture insert surface area (60 mm^2). Three measurements per insert were performed, and three inserts per condition were used. Inserts without cells were used as blanks.

Permeability Assay

After the TEER measurement assay, CECs cultured on inserts were used for permeability measurements. At 7 days post-confluence, 40 µg/mL 4-kDa dextran–FITC (Sigma-Aldrich) or 10-kDa dextran–Alexa Fluor 488 (Sigma-Aldrich) was added to the inserts and incubated in the dark at 37°C. After 2.5 hours, the medium below the insert was collected, and the fluorescence was measured at 530 nm with a CytoFluor 4000 Plate Reader (Life Technologies). Each condition was performed in duplicate, and five reads per condition were captured. Fluorescence was normalized to the fluorescence from an insert without cells. CECs on inserts were then fixed in 4% paraformaldehyde for indirect immunostaining.

Western Blotting

Total proteins were harvested at 7 days postconfluence with radioimmunoprecipitation assay buffer supplemented with a cocktail of phosphatase inhibitors, protease inhibitors and phenylmethanesulfonyl fluoride. After 30 minutes on ice, the extracts were centrifuged. Supernatants were collected and stored at −80°C. The protein concentration was determined with a Pierce Micro BCA Protein Assay Kit (Thermo Fisher Scientific) according to the manufacturer's instructions.

For western blotting, proteins were diluted to 1 µg/µL in Laemmli buffer and denatured at 95°C for 5 minutes. Samples were run on 7.5% acrylamide gels at 100 V for 90 minutes and transferred at 120 V for 90 minutes. The membranes were blocked in 5% nonfat powdered milk diluted in Tris-buffered saline (TBS) containing 0.5% Tween 20 (Promega, Madison, WI, USA) for 1 hour. The primary antibody (mouse monoclonal anti-N-cadherin; Agilent Technologies) was added to the membranes and incubated overnight at 4°C on a shaking platform. The membranes were then washed three times with TBS–Tween 20. Then, the secondary antibody (peroxidase-conjugated AffiniPure Goat Anti-Mouse Antibody; Thermo Fisher Scientific) was added and incubated for 1 hour at room temperature. The membranes were visualized using enhanced chemiluminescent substrate (Western Sure Premium Chemiluminescent Substrate; Li-COR, Lincoln, NE, USA) and a scanner (C-Digit Chemiluminescence Western Blot Scanner; Li-COR). Tubulin served as a loading control (mouse anti-α-tubulin antibody; Abcam, Cambridge, UK). Relative quantification of the western blotting bands was performed using Li-COR Image Studio Digits software. The means of the measurements for each sample and standard deviations were calculated using Excel (Microsoft, Redmond, WA, USA). The results are presented as the protein relative to the loading control.

TGF-β Phospho Antibody Array

The TGF-β Phospho Antibody Array (Full Moon BioSystems, Sunnyvale, CA, USA) is an ELISA-based assay featuring 176 antibodies against proteins associated with the TGF-β signaling pathway. Protein extracts were obtained following the manufacturer's protocol for adherent cells. Lysates were purified, quantified (absorbance at 280 nm), and biotinylated prior to their addition to the precoated slides. The protein concentration was 4 mg/mL. A Cy3-coupled antibody against biotin was used for detection. The slides were read with a SureScan Microarray scanner (Agilent Technologies) and analyzed using ImageJ.

Gene Profiling

After 1 week of culture in maturation media supplemented with or without TGF-β2, CECs were harvested and flash-frozen at −80°C. RNA isolation was performed with an

RNeasy Mini Kit (QIAGEN, Hilden, Germany) following the manufacturer's protocol. The quantity and quality of RNA (RNA integrity number) were assessed with an Agilent Technologies 2100 bioanalyzer and RNA 6000 Nano LabChip Kit. Only samples with an RNA integrity number over 7 were used for gene profiling. Gene profiling was performed by the CUO-Recherche gene profiling service (Québec, QC, Canada) using Agilent Technologies' protocol. Briefly, cRNA was labeled with cyanine 3-CTP using the Agilent One-Color Microarray-Based Gene Expression Analysis Kit (Agilent Technologies). Then, 600 ng of cRNA was incubated on a G4851A SurePrint G3 Human GE 8 × 60K microarray slide (60,000 probes; Agilent Technologies) for cRNA hybridization. The slide was washed and scanned on an Agilent SureScan Scanner. The data were extracted with Arraystar V12 software (DNASTAR, Madison, WI, USA) and transformed into log2 values.

The microarray linear expression data were uploaded into Network Analyst (https://www.networkanalyst.ca/) to be filtered and normalized (variance-stabilizing normalization). A list of significantly differentially expressed genes (Benjamini–Hochberg adjusted $P < 0.05$ and log fold change >1.0) was then generated using the limma statistical method (Supplementary Material). This list was then used to generate causal gene interaction networks related to selected cellular functions of interest in CECs exposed to TGF-β2.

Adhesion Assay

After 1 week of culture in maturation media supplemented with or without TGF-β2, CECs were harvested and resuspended in M-medium at 10 million cells/mL. Human corneas ($N = 5$ pairs) were devitalized using three freeze–thaw cycles and washed to remove the native endothelial cells, resulting in a bare Descemet's membrane.[15] The devitalized corneas were then mounted on a corneal bioreactor.[11] Each bioreactor was connected to a 60-mL syringe inserted into a syringe pump that was set to inject M-medium at a rate of 5 µL/min. The disposal bottle was placed high enough to generate a pressure between 16 and 21 mmHg. Then, 100 µL (10^6 CECs) was injected with a 30-gauge needle through the peripheral cornea. The mounted corneas were turned upside-down (epi-side down) for 3 hours in order for the CECs to adhere to the Descemet's membrane, then returned to their epi-side-up position. The dynamic cultures were maintained for 2 or 7 days. The nonadherent cells were eliminated via the flow of M-medium into the disposal bottle. At the end of the experiment, the corneas were carefully demounted, and Alizarin Red staining was performed as described.[15] Images were analyzed using ImageJ to calculate endothelial cell density. The endothelium was further fixed with 4% paraformaldehyde, and indirect immunofluorescence was performed to visualize cell–cell junctions (zonula occludens-1 [ZO-1] and N-cadherin) as described above.

Statistical Analysis

The results are presented as the mean of all measurements and standard error of the mean. Statistical significance was calculated with one- or two-way ANOVAs, followed by Tukey's multiple comparisons test using Prism 7 (GraphPad, San Diego, CA, USA). $P < 0.05$ was considered significant.

Data Availability

The gene expression data were deposited in the Gene Expression Omnibus (GEO) database (http://www.ncbi.nlm.nih.gov/geo/; accession number GSE172573).

Results

Evaluation of the Effects of TGF-β Isoforms on CEC Morphology

We first evaluated whether all three TGF-β isoforms influenced cell morphology when added during the maturation phase of postconfluent CECs. After the cells reached confluence, the growth media were replaced with maturation media containing (or not) TGF-β1, TGF-β2, or TGF-β3 for 7 days, and phase-contrast images were obtained at every medium change. The effect of TGF-β on cell morphology was slowly progressive (Supplementary Fig. S1). After 7 days, CECs cultured in maturation medium without TGF-β exhibited a more elongated cell morphology, whereas cells cultured in the presence of TGF-β1, -β2 and -β3 were more polygonal (Fig. 1A). This observation was supported by the mean CI (Fig. 1B). Indeed, the CI of the control condition was 0.57 ± 0.16. The CI increased when CECs were matured in the presence of the TGF-β isoforms, especially TGF-β2, and these cells exhibited an endothelial/polygonal cell morphology (TGF-β1, CI = 0.67 ± 0.13; TGF-β2, CI = 0.71 ± 0.12; TGF-β3, CI = 0.65 ± 0.13).

Effect of TGF-β Isoforms on Intercellular Junction Protein Expression

The levels of the intercellular junction-related proteins ZO-1, β-catenin, and N-cadherin were observed by immunofluorescence microscopy 7 days postconfluence (Fig. 1A). In the control condition, ZO-1 and β-catenin were scattered within the cytoplasm (Fig. 1A, second and third column). When TGF-β isoforms were added, these proteins were present at the cell membrane. N-cadherin was absent in the control condition (Fig. 1A, fourth column), but its protein expression increased after incubation with all three TGF-β isoforms. This increase in N-cadherin expression was confirmed by western blotting (Figs. 1C, 1D). The relative expression increased from 4.9 to 5.6 times that of the control when TGF-β was added (Fig. 1D).

In Vitro Functionality of CECs Exposed to TGF-β1, TGF-β2, and TGF-β3.

TEER measures the integrity of a monolayer. TEER measurements were performed at every medium change after confluence (Fig. 2A). At the first medium change (confluence), CECs had similar TEER values under all conditions (control, 11.7 ± 5.6 Ωcm^2; TGF-β1, 12.0 ± 5.6 Ωcm^2; TGF-β2, 14.5 ± 5.2 Ωcm^2; TGF-β3, 14.2 ± 6.9 Ωcm^2). Then, TEER increased throughout the maturation period. At the second time point (t2), the CECs exposed to TGF-β1 (24.1 ± 5.9) and TGF-β2 (25.0 ± 5.2) had significantly higher TEER values than the CECs exposed to the control condition (16.1 ± 5.9 Ωcm^2). At t3, only the CECs exposed to the TGF-β2 condition (31.5 ± 6.7 Ωcm^2) had significantly higher TEER than the CECs exposed to the control condition (22.3 ± 9.8). At 7 days postconfluence, there was no significant difference between the CECs exposed to all of the conditions (control,

Investigative Ophthalmology & Visual Science

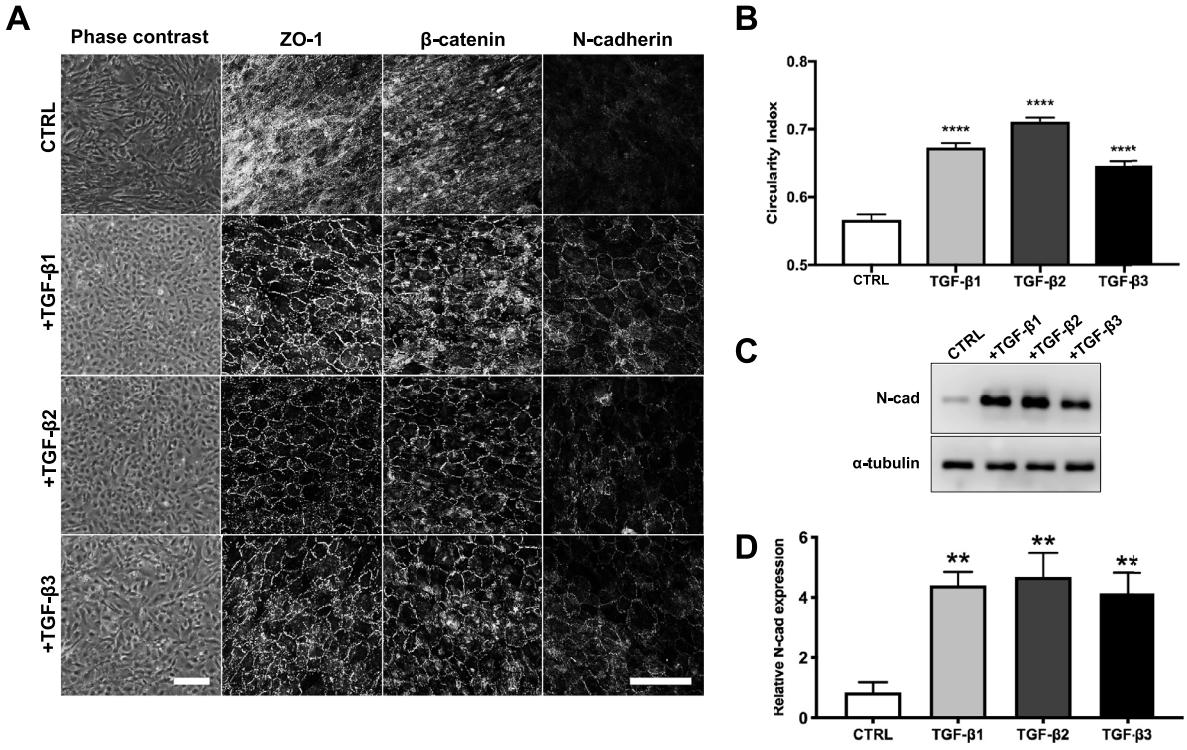

Figure 1. Effect of TGF-β1, TGF-β2, and TGF-β3 on cell morphology and junctional complexes. (**A**) Representative images of phase-contrast images (*first column*) and immunofluorescence detection of ZO-1 (*second column*), β-catenin (*third column*), and N-cadherin (*fourth column*) at day 7 postconfluence in control maturation medium (CTRL; *first line*) or in maturation medium containing TGF-β1 (*second line*), TGF-β2 (*third line*), or TGF-β3 (*fourth line*). *Scale bar*: 100 µm (phase-contrast and immunofluorescence images). (**B**) CI calculated from the area and perimeter for all conditions. (**C**) Representative western blots against N-cadherin (α-tubulin as loading control). (**D**) Bar graph of relative quantification of N-cadherin for all conditions. Results are expressed with mean ± SEM. $^{**}P < 0.005$; $^{****}P < 0.0001$.

27.9 ± 6.3 Ωcm^2; TGF-β1, 27.0 ± 6.7 Ωcm^2; TGF-β2, 33.4 ± 6.2 Ωcm^2; TGF-β3, 29.0 ± 4.1 Ωcm^2), but all of these cells showed a significant increase in TEER compared to the first measurement (Fig. 2B). Acute retinal pigment epithelial 19 (ARPE-19) cells were used as a positive control (cells that consistently form an efficient barrier with a high TEER) (Fig. 2B, 63.9 ± 4.1 Ωcm^2). Fibroblasts were used as a negative control because they do not form a well-organized barrier and maintain a low TEER (Fig. 2B, 21.4 ± 1.9 Ωcm^2).

The fact that TEER increased in fibroblasts, which do not form a cell monolayer, led us to wonder if the increase in TEER could be due to a superposition of cells rather than an increase in barrier integrity. To confirm the implication of cell–cell junctions in the TEER measurements, further TEER analysis was performed using a Ca^{2+}-switch assay (Fig. 2C). This assay is based on the requirement of calcium for junction protein conformation.[2] When calcium is removed from the culture medium, a decrease in TEER is observed for cells that have previously formed intercellular junctions. CECs without TGF-β (control condition) showed no variation in TEER during the Ca^{2+}-switch assay. This demonstrates that these fibroblast-like cells TEER values were not obtained because of the presence of intercellular junctions but rather because they formed a physical barrier due to a stacking of cells growing on top of each other. The TEER values from the three TGF-β treatment groups decreased (approximately 50%) when calcium was depleted from the medium. When Ca^{2+} was added back, the TEER measurements increased after 60 minutes in all of the TGF-β treatment groups, indicating the importance of their intercellular junctions. The junction-related protein ZO-1 was also correctly cytolocalized near the cell membrane 60 minutes after Ca^{2+} was added back to the culture media (Fig. 2D).

Permeability tests were also performed on 7-day postconfluent CECs using dextran (4 and 10 kDa) coupled to a fluorescent dye (Fig. 2E). The control group had a nonsignificantly higher percentage of 4-kDa dextran permeability than the TGF-β–treated groups. There was no difference in the percentage of 10-kDa dextran permeability under any of the four conditions. ARPE-19 cells and fibroblasts were used as positive and negative controls, respectively. Because treatment with TGF-β2 resulted in the greatest increase in CI (Fig. 1B) and faster recovery of in vitro barrier integrity (Fig. 2A), we performed the remaining experiments using only TGF-β2.

Gene Profiling and Signaling Pathway Profiling of CECs Exposed to TGF-β2

To obtain a better understanding of the effect of TGF-β during cell maturation, we performed a wide gene expression analysis, as well as signaling pathway activation analysis, with a TGF-β–specific array. Gene profiling analysis showed that 332 gene products were deregulated by twofold following maturation with TGF-β2 (170 genes were upregulated and 162 genes were downregulated) (Fig. 3A). With these deregulated genes, we performed a functional analysis using NetworkAnalyst. Principal component analysis showed that the four investigated CEC populations cultured

Investigative Ophthalmology & Visual Science

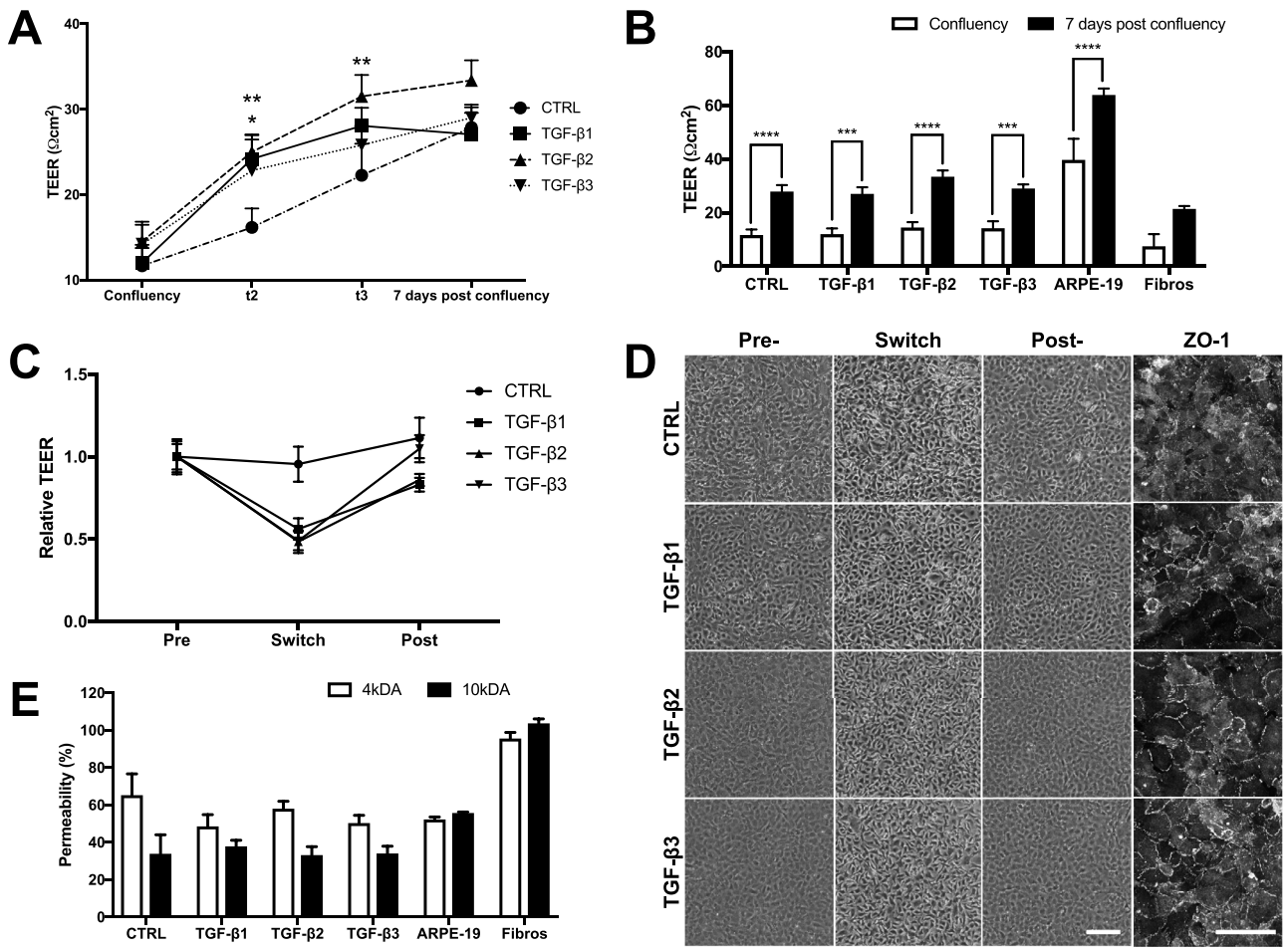

Figure 2. In vitro functionality of corneal endothelial cells through cell maturation with TGF-β1, TGF-β2, and TGF-β3. (**A**) TEER measurements through cell maturation of endothelial corneal cells that matured in control medium (CTRL) or in medium containing TGF-β1, TGF-β2, or TGF-β3. (**B**) TEER measurements at confluence and at day 7 postconfluence for all conditions. The ARPE-19 cell line was used as high TEER control and fibroblasts (fibros) as low TEER control. (**C**) Relative TEER during Ca^{2+}-switch assay. (**D**) Phase-contrast images of CECs before (pre), during (switch), and after (post) Ca^{2+}-switch assay and ZO-1 staining after Ca^{2+}-switch assay. *Scale bar*: 100 µm (phase-contrast and immunofluorescence images). (**E**) Permeability percentage of 4-kDa and 10-kDa dextran for all conditions including control (ARPE-19 and fibros). $^{**}P < 0.005$; $^{***}P < 0.0005$; $^{****}P < 0.0001$.

with TGF-β2 had a more uniform transcriptome than the control CECs, which exhibited high gene expression variability among individual samples (Fig. 3B). Functional analysis revealed that genes that were the most upregulated by TGF-β2 were associated with focal adhesion and extracellular matrix (ECM)–receptor interactions (Fig. 3C).

At the level of intercellular junction-related genes, only the expression of *CDH2* was dysregulated after incubation with TGF-β2 (Fig. 4A). Indeed, the expression of *CDH2*, which encodes N-cadherin, was upregulated (4×; $P = 0.01$) by TGF-β2, which is in accordance with the upregulated protein level. Among ECM-related genes, we identified *COL4A1*, *COL4A2*, *COL4A4*, *COL8A1*, and *COL8A2* as exhibiting significantly upregulated expression in TGF-β2–treated CECs (Fig. 4B). *SLC4A11*, known to participate in CEC adhesion,[16] was also significantly upregulated with TGF-β2 (2.1×; $P = 0.048$) (Fig. 4B).

Signaling pathway activation was assessed with a TGF-β Phospho Antibody Array (Figs. 4C, 4D). We found eight upregulated phosphorylated proteins, including protein kinase B (AKT; phospho-Ser473, 4.5×), mammalian target of rapamycin (mTOR; phospho-Ser2448, 5.5×; phospho-Ser-2481, 5.4×), S6 ribosomal protein (phospho-Ser235, 6×), p38 mitogen-activated protein kinase (MAPK; phospho-Thr180, 5×), specificity protein 1 (SP1; phospho-Thr739, 13.7×), extracellular signal-regulated kinase 1 (ERK1)-p44/42 MAPK (phospho-Tyr204, 6.1×), and mothers against decapentaplegic homolog 3 (Smad3; phospho-Ser425, 2.4×). Four proteins were phosphorylated to lesser degrees, including MAPK kinase 3 (MKK3; phospho-Ser189, 0.3×), MKK3/MAP2K3 (phospho-Thr222, 0.06×), SAPK/Erk kinase (SEK1)/MMK4 (phospho-Thr261, 0.1×), and Ras-guanine nucleotide releasing factor 1 (GRF1; phospho-916, 0.4×).

Adhesion of CECs on Devitalized Descemet's Membranes

We evaluated the increased cell-substrate adhesion by injecting cells onto the bare Descemet's membrane of ex vivo corneas mounted on a corneal bioreactor (Fig. 5A). One million CECs that were matured in the presence (or absence)

Investigative Ophthalmology & Visual Science

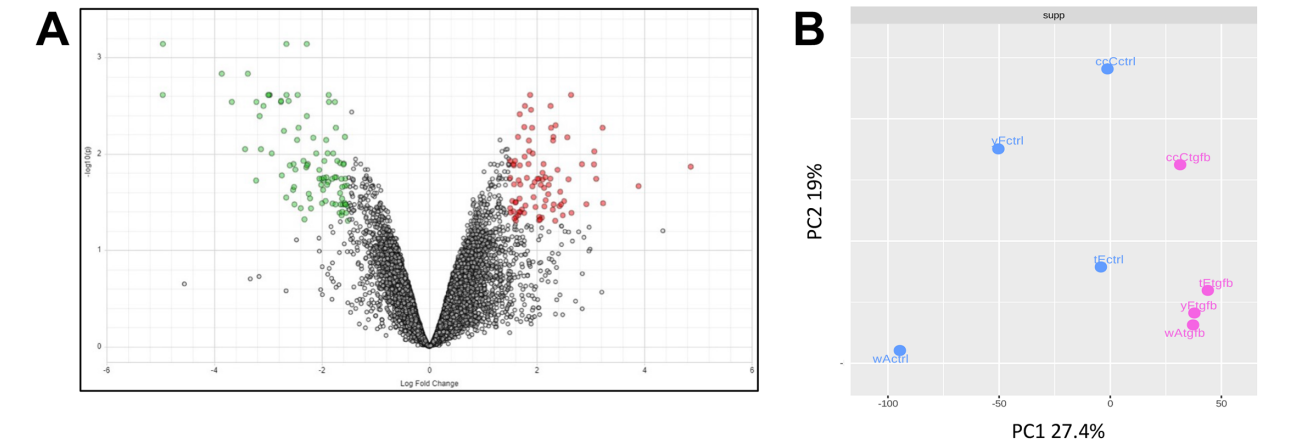

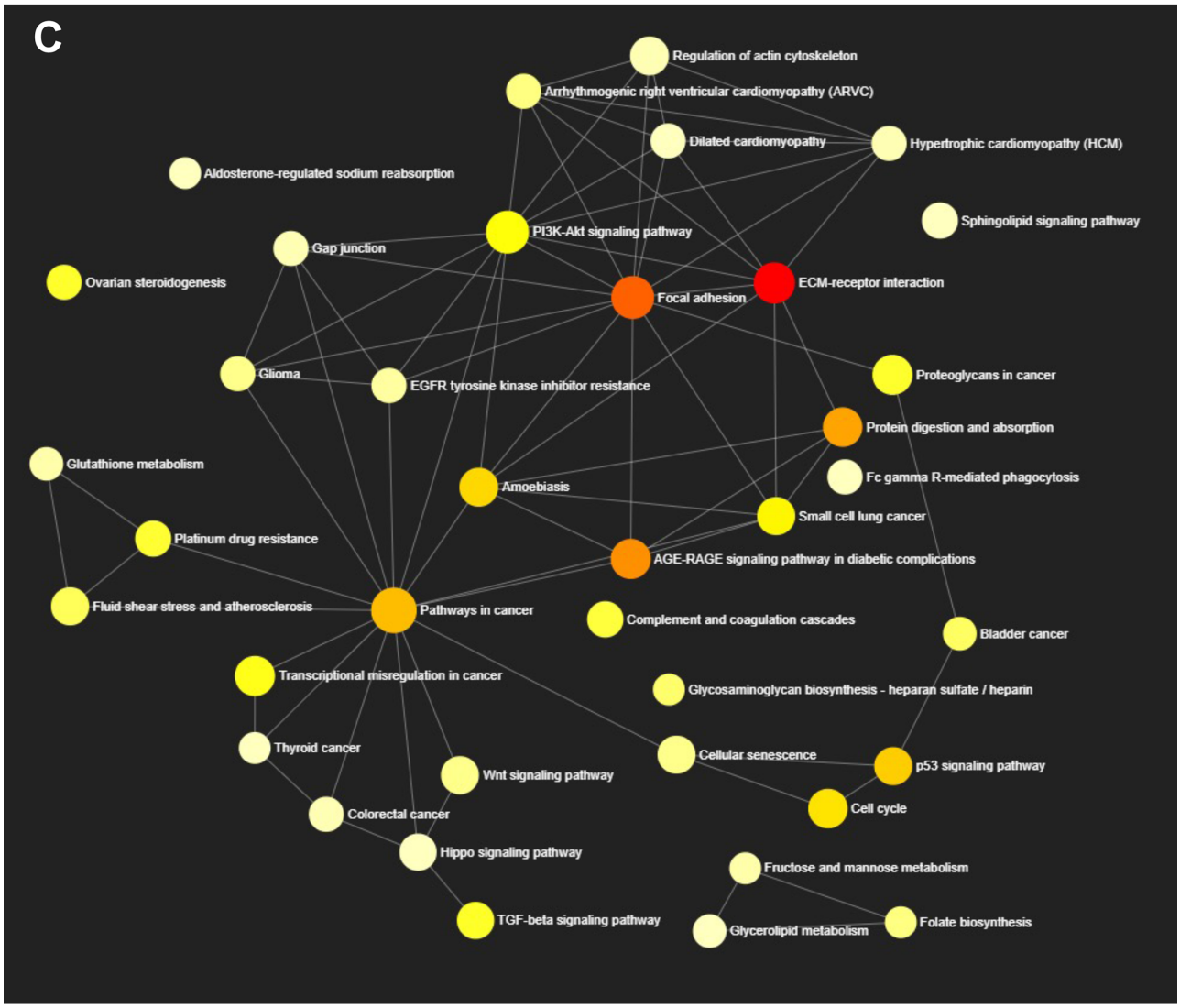

Figure 3. Gene and activated signaling pathway profiles of CECs that matured in the presence of TGF-β2. (**A**) Volcano plot of *P* values presented as log2 of linear expression for all genes. (**B**) Principal component analysis. *Blue dots* represent the four populations in the CTRL condition, and *pink dots* represent the four populations that matured with TGF-β2. (**C**) Functional analysis where each dot represents a cellular function. *Dot colors* represent the strength of the correlation (e.g., *red* means that gene expression strongly correlates with the function). Links between the dots represent close relations between the functions.

Investigative Ophthalmology & Visual Science

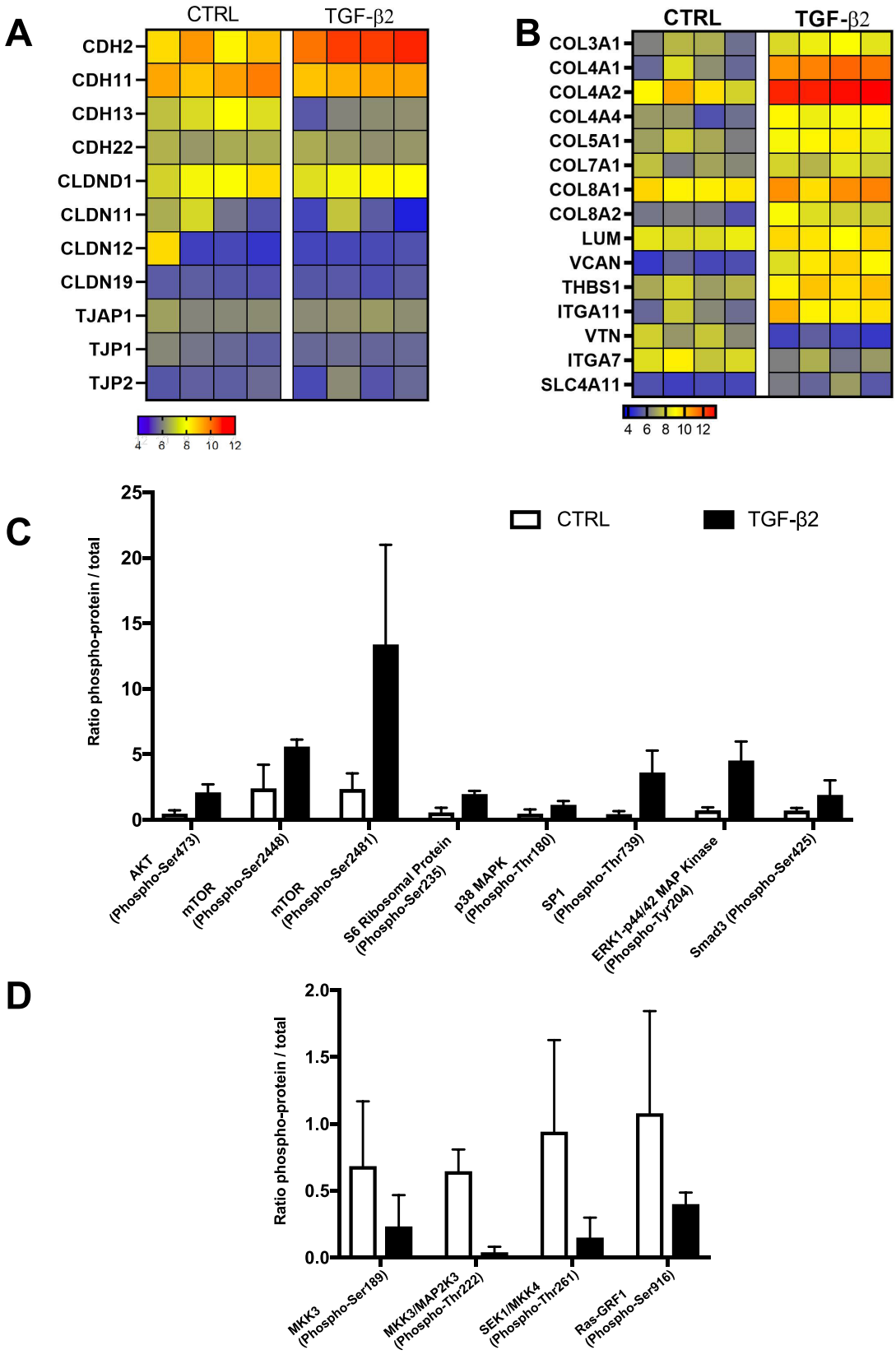

Figure 4. Changes in gene expression or kinase activation after 7 days of maturation with TGF- β2. (**A**) Heat map of differently expressed intercellular-related genes. *CDH* genes are genes encoding for cadherins (adherens junctions); *CLDN*, *TJAP1*, *TJP1*, and *TJP2* are tight junction-related genes. (**B**) Heat map of differentially expressed adhesion-related genes. The first eight genes are collagen-related genes;

Investigative Ophthalmology & Visual Science

LUM and *VCAN* are proteoglycan-related genes, *VTN* and *THBS1* are glycoprotein-related genes, and *ITGA11* and *ITGA7* are genes encoding for integrins. *SLC4A11* encodes for a Na^+-coupled OH^- transporter,[57] and the protein has been shown to play a role in CEC adhesion to Descemet's membrane.[16] (**C**, **D**) TGF-β Phospho Antibody Array analysis of upregulated protein activation (**C**) and downregulated protein activation (**D**).

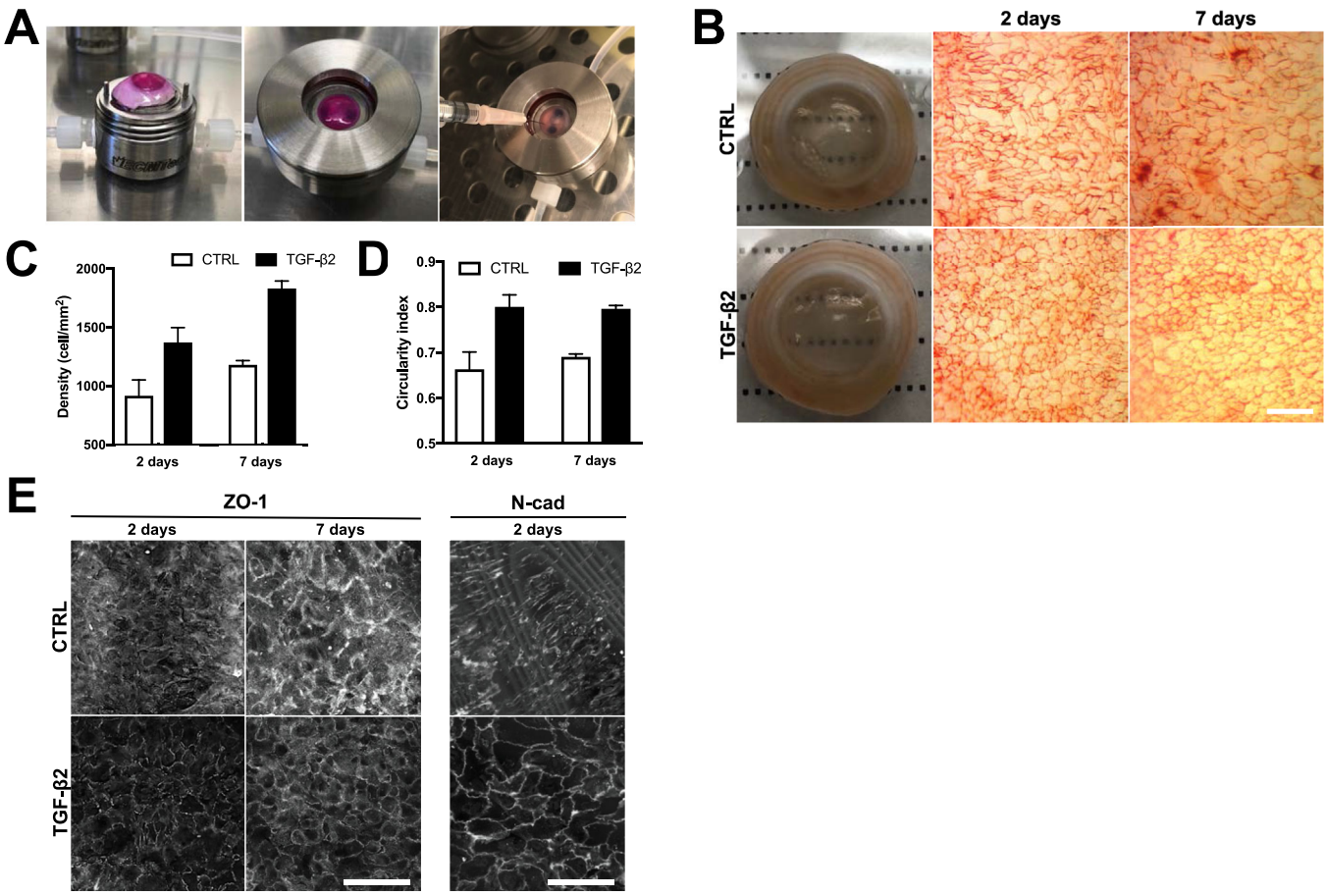

Figure 5. Adhesion assay after cell maturation with TGF-β2. (**A**) Pictures of the corneal bioreactor with a devitalized cornea and cell injection procedure. (**B**) Macroscopic and Alizarin Red staining images of corneas after dynamic culture. *Scale bar*: 100 µm (Alizarin Red images). (**C**) Bar graph of cell density on Descemet's membrane after dynamic culture. (**D**) Bar graph of circularity indexes. (**E**) Representatives images of immunofluorescence detection of ZO-1 and N-cadherin. *Scale bar*: 100 µm.

of TGF-β2 were injected into the anterior chamber and incubated under pressure for 2 or 7 days. After 2 days of dynamic culture, both conditions generated clear corneas (Fig. 5B). Alizarin Red staining revealed that CECs that were matured with TGF-β2 formed an endothelium with a higher endothelial cell density (2 days, 1372 $\pm$ 219 cells/mm^2; 7 days, 1832 $\pm$ 90 cells/mm^2) than the control CECs (2 days, 917 $\pm$ 235 cells/mm^2; 7 days, 1180 $\pm$ 50 cells/mm^2) (Figs. 5B, 5C). TGF-β2–matured CECs also had a higher CI after 2 days (control, 0.66 $\pm$ 0.04; TGF-β2, 0.80 $\pm$ 0.03) and 7 days (control, 0.69 $\pm$ 0.006; TGF-β2, 0.79 $\pm$ 0.007) of dynamic culture (Fig. 5D). CECs that were matured in the presence of TGF-β2 had membrane-bound ZO-1 after only 2 days of dynamic culture, whereas control CECs had less ZO-1 bound at the membrane after 7 days of dynamic culture (Fig. 5E). The same pattern was observed with N-cadherin at 2 days of dynamic culture (Fig. 5E).

Discussion

The corneal endothelium plays an important role in maintaining corneal stromal transparency, and it achieves this transparency through a fragile "pump–leak" balance. Understanding how CECs form intercellular junctions is thus important to comprehending how they maintain their barrier integrity in health and disease states. It is known that all three TGF-β isoforms are found in normal aqueous humor.[10,17] Studying their impact on CECs allows for a better comprehension of CEC biology. In this study, we first showed that all three TGF-β isoforms, when added to post-confluent CECs, influenced cell morphology, cell–cell junction protein expression, and endothelial barrier integrity (TEER).

The isoform that is most concentrated in the healthy aqueous humor is TGF-β2. Depending on reports, its total

Investigative Ophthalmology & Visual Science

amount ranges from 100 to 8000 pg/mL, and the amount of its active form ranges from 40 to 5000 pg/mL.[10,18–36] TGF-β2 was reported to play a role in the growth arrest of CECs in vitro.[37–39] It has also been reported to help maintain the immune privilege of the anterior chamber.[40] Isoform 2 of TGF-β is the major isoform implicated in anterior chamber development at the embryonic stage.[41] TGF-β1 is present at lower concentrations than TGF-β2 in healthy aqueous humor (total, 5–100 pg/mL; active, 0–5 pg/mL),[19,24–26,28,32,33,42,43] whereas TGF-β3 is nearly absent.[19,24–26,28] Their roles in CEC biology are not well understood. In other layers of the cornea, TGF-β1 is involved in cell migration[44] and ECM production by keratocytes.[45] TGF-β3 is known to induce cell proliferation in epithelial wound repair[46] and to have antifibrotic proprieties by promoting normal ECM assembly by fibroblasts in keratoconus.[47]

All three active TGF-β isoforms, when added during the maturation phase (when cells have stopped proliferating), increased the formation of intercellular junctions. Because cell–cell junction formation is known to be a cause of growth arrest,[48] our results suggest that the effect of TGF-β on growth arrest might be mediated through cell junction reorganization. TGF-β isoforms may be important in the maintenance of the barrier integrity of the corneal endothelium, as they restore in vitro functionality. Ca^{2+}-switch assays have shown that only CECs exposed to TGF-β reached TEER that is similar to that of mature junctions.[49] Ca^{2+} is a major regulator of cadherin conformation, which also influences tight junction assembly.[49,50] Control CECs showed no change in TEER after Ca^{2+} depletion, confirming the low expression of N-cadherin, as well as the delocalization of ZO-1 and β-catenin observed via immunofluorescence staining. Here, our results revealed that junction assembly was accelerated when TGF-β1, TGF-β2, or TGF-β3 was added to maturation media, a finding that is consistent with our previous work on TGF-β1[9] and suggests an important role for this cytokine in CEC homeostasis.

The analysis of the signaling pathways that are activated in the presence of TGF-β2 revealed 12 proteins that were up- or downregulated by at least twofold. Among the activated proteins, Smad3[51,52] and AKT[53] are known to be involved in increasing N-cadherin expression, which correlates with our results at both the gene and protein levels. Homotypic binding of N-cadherin is the first step in intercellular junction formation.[54] After the establishment of a strong interaction between cadherins of neighboring cells, other proteins linked to the junctional complex are scaffolded. Initiating the expression of N-cadherin is therefore important to obtain a mature endothelium, ensuring its barrier function.

Gene profiling provided insights into the deregulated gene expression that we further analyzed. Principal component analysis showed that adding TGF-β2 decreased interindividual variations by clustering the populations, making CEC culture outcomes more constant. Functional analysis demonstrated that TGF-β2 increased the transcription of the collagens that are present in the basal membrane of the corneal endothelium (Descemet's membrane), such as collagen types IV and VIII, and increased the transcription of integrins that bind to laminin and collagens (also components of Descemet's membrane[55,56]), suggesting that this cytokine influences cell–ECM interactions; this result was confirmed by the QIAGEN Ingenuity Pathway Analysis. A new player in CEC adhesion is solute carrier family 4 member 11 (SLC4A11), a Na^+-coupled OH^- transporter[57] that has recently been shown to play a role in CEC adhesion to Descemet's membrane.[16] Following 1 week postconfluence, TGF-β2 induced a twofold increase in *SLC4A11* gene expression. This result is consistent with a previous paper that reported a 17-fold increase in *SLC4A11* gene expression following 4 weeks of postconfluence,[58] also suggesting that, after 7 days with TGF-β, CECs would therefore be at an early stage of maturation and would benefit from a longer maturation time.

Although we did not study ECM deposition, our gene profiling analysis suggests that TGF-β2 increases ECM deposition in CECs. Consistent with this hypothesis, Ignotz et al.[59] reported an increase in the production of ECM (fibronectin and collagens) when CECs were exposed to TGF-β1. Moreover, in lens epithelial cells, TGF-β has been reported to increase cell–ECM interactions via a process mediated by Rho and Rac GTPase activation.[60] Cell–ECM interactions similarly activate many signaling pathways that reshape the actin cytoskeleton.[61] These signaling pathways, such as phosphatidylinositol-3-kinase (PI3K)/AKT, which were activated in our CECs that were matured with TGF-β2, also play a role in tight and adherent junction establishment.[62,63] Taken together, our results suggest that the enhanced barrier functionality, revealed by cell–cell junction expression and TEER measurements, could occur secondary to the increased adhesion of CECs to their substrate following TGF-β exposure.

When we performed the adhesion assay, we found that the cell density was higher when CECs had matured in TGF-β2–supplemented medium, suggesting that more CECs adhered to the devitalized Descemet's membrane. Additionally, our results suggest better barrier functionality, which was demonstrated by increased expression and better cytolocalization of ZO-1 and N-cadherin.

TGF-β controls many fundamental aspects of cellular behavior. It can promote endothelial to mesenchymal transition (EndMT) in subconfluent CECs,[9] and adding the TGF-β receptor inhibitor SB451542 during the cell culture process has been shown to reduce the development of EndMT that can occur during subculture.[64] Serial passaging has also been shown to increase senescent-associated changes, such as activation of the p38 MAPK pathway,[65] a pathway that was also more activated in the presence of TGF-β herein. Given that we used P3 cultures, we cannot exclude that a side population of cells could have been in a senescent or subsenescent state. Performing the experiment using P0 or P1 cultures would reduce this limitation. Demonstration that P0 or P1 cells would respond similarly to P3 cells remains to be performed.

It has been shown that TGF-β acts as an antiproliferating agent in cultured CECs, mediated by p27kip1 (a G1-phase inhibitor), suggesting that TGF-β could be one of the pathways that lead to G1 phase arrest in CECs in vivo.[37,38,66] It would make sense, in the context of our study using postconfluent maturing CECs, that a mitotic inhibition generated by TGF-β would help establish stable cell–cell and cell–substrate contacts, which in turn would generate a more functional monolayer.

In conclusion, this study shows that adding TGF-β2 to postconfluent maturing P3 CECs increases intercellular junction formation, improves in vitro barrier functionality, and increases cell–ECM interactions. This represents a step forward in better understanding CEC biology.

Investigative Ophthalmology & Visual Science

Acknowledgments

The authors thank the CUO Eye Bank's personnel for ongoing collaboration and Mathieu Thériault for technical assistance, as well as Gaëtan Le-Bel and Sylvain Guérin for the microarrays.

Supported by a grant from the Natural Sciences and Engineering Research Council of Canada (RGPIN-2018-06268 to SP). Procurement of eyes and corneas for research from the CUO Eye bank was possible thanks to an infrastructure grant from the Vision Health Research Network (to SP) and KS and SCG were FRQ-S scholars and KS also received a travel grant from the ThéCell Network, a network supported by the "Fonds de recherche du Québec–Santé."

Disclosure: **K. Santerre**, None; **S. Cortez Ghio**, None; **S. Proulx**, None

References

1. He Z, Forest F, Gain P, et al. 3D map of the human corneal endothelial cell. *Sci Rep*. 2016;6:29047.
2. Srinivas SP. Dynamic regulation of barrier integrity of the corneal endothelium. *Optom Vis Sci*. 2010;87:E239–E254.
3. Bonanno JA. Molecular mechanisms underlying the corneal endothelial pump. *Exp Eye Res*. 2012;95:2–7.
4. Bahn CF, Glassman RM, MacCallum DK, et al. Postnatal development of corneal endothelium. *Invest Ophthalmol Vis Sci*. 1986;27:44–51.
5. Bourne WM, Nelson LR, Hodge DO. Central corneal endothelial cell changes over a ten-year period. *Invest Ophthalmol Vis Sci*. 1997;38:779–782.
6. Yee RW, Matsuda M, Schultz RO, Edelhauser HF. Changes in the normal corneal endothelial cellular pattern as a function of age. *Curr Eye Res*. 1985;4:671–678.
7. Zhu YT, Hayashida Y, Kheirkhah A, He H, Chen SY, Tseng SC. Characterization and comparison of intercellular adherent junctions expressed by human corneal endothelial cells in vivo and in vitro. *Invest Ophthalmol Vis Sci*. 2008;49:3879–3886.
8. Hamuro J, Toda M, Asada K, et al. Cell homogeneity indispensable for regenerative medicine by cultured human corneal endothelial cells. *Invest Ophthalmol Vis Sci*. 2016;57:4749–4761.
9. Beaulieu Leclerc V, Roy O, Santerre K, Proulx S. TGF-β1 promotes cell barrier function upon maturation of corneal endothelial cells. *Sci Rep*. 2018;8:4438.
10. Jampel HD, Roche N, Stark WJ, Roberts AB. Transforming growth factor-β in human aqueous humor. *Curr Eye Res*. 1990;9:963–969.
11. Theriault M, Roy O, Brunette I, Proulx S. Physiological pressure enhances the formation of tight junctions in engineered and native corneal endothelium. *Exp Eye Res*. 2019;179:102–105.
12. Santerre K, Xu I, Thériault M, Proulx S. In vitro expansion of corneal endothelial cells for transplantation. *Methods Mol Biol*. 2020;2145:17–27.
13. Peh GS, Chng Z, Ang HP, et al. Propagation of human corneal endothelial cells: a novel dual media approach. *Cell Transplant*. 2015;24:287–304.
14. Xu I, Thériault M, Brunette I, Rochette PJ, Proulx S. Matrix metalloproteinases and their inhibitors in Fuchs endothelial corneal dystrophy. *Exp Eye Res*. 2021;205:108500.
15. Proulx S, Audet C, Uwamaliya J, et al. Tissue engineering of feline corneal endothelium using a devitalized human cornea as carrier. *Tissue Eng Part A*. 2009;15:1709–1718.
16. Malhotra D, Jung M, Fecher-Trost C, et al. Defective cell adhesion function of solute transporter, SLC4A11, in endothelial corneal dystrophies. *Hum Mol Genet*. 2020;29:97–116.
17. Cousins SW, McCabe MM, Danielpour D, Streilein JW. Identification of transforming growth factor-beta as an immunosuppressive factor in aqueous humor. *Invest Ophthalmol Vis Sci*. 1991;32:2201–2211.
18. Stadnikova A, Dudakova L, Skalicka P, Valenta Z, Filipec M, Jirsova K. Active transforming growth factor-β2 in the aqueous humor of posterior polymorphous corneal dystrophy patients. *PLoS One*. 2017;12:e0175509.
19. Matthaei M, Gillessen J, Muether PS, et al. Epithelial–mesenchymal transition (EMT)-related cytokines in the aqueous humor of phakic and pseudophakic Fuchs' dystrophy eyes. *Invest Ophthalmol Vis Sci*. 2015;56:2749–2754.
20. Trivedi RH, Nutaitis M, Vroman D, Crosson CE. Influence of race and age on aqueous humor levels of transforming growth factor-beta 2 in glaucomatous and nonglaucomatous eyes. *J Ocul Pharmacol Ther*. 2011;27:477–480.
21. Guo T, Guo L, Fan Y, et al. Aqueous humor levels of TGFβ2 and SFRP1 in different types of glaucoma. *BMC Ophthalmol*. 2019;19:170.
22. de Boer JH, Limpens J, Orengo-Nania S, de Jong PT, La Heij E, Kijlstra A. Low mature TGF-beta 2 levels in aqueous humor during uveitis. *Invest Ophthalmol Vis Sci*. 1994;35:3702–3710.
23. Zhu XJ, Chen MJ, Zhang KK, Yang J, Lu Y. Elevated TGF-β2 level in aqueous humor of cataract patients with high myopia: potential risk factor for capsule contraction syndrome. *J Cataract Refract Surg*. 2016;42:232–238.
24. Yoneda K, Nakano M, Mori K, Kinoshita S, Tashiro K. Disease-related quantitation of TGF-beta3 in human aqueous humor. *Growth Factors*. 2007;25:160–167.
25. Cao Q, Xiao B, Jin G, et al. Expression of transforming growth factor β and matrix metalloproteinases in the aqueous humor of patients with congenital ectopia lentis. *Mol Med Rep*. 2019;20:559–566.
26. Garweg JG, Zandi S, Gerhardt C, Pfister IB. Isoforms of TGF-β in the aqueous humor of patients with pseudoexfoliation syndrome and a possible association with the long-term stability of the capsular bag after cataract surgery. *Graefes Arch Clin Exp Ophthalmol*. 2017;255:1763–1769.
27. Maier P, Broszinski A, Heizmann U, Boehringer D, Reinhard T. Determination of active TGF-β_2 in aqueous humor prior to and following cryopreservation. *Mol Vis*. 2006;12:1477–1482.
28. Chen Y, Yan H, Li G, Zhang Y. Higher TGF-β1, TGF-β2, MMP-2, and TIMP-1 levels in the aqueous humor of patients with acute primary angle closure. *Ophthalmic Res*. 2021;64:62–67.
29. Jia Y, Hu DN, Zhou J. Human aqueous humor levels of TGF-β2: relationship with axial length. *Biomed Res Int*. 2014;2014:258591.
30. Ozcan AA, Ozdemir N, Canataroglu A. The aqueous levels of TGF-beta2 in patients with glaucoma. *Int Ophthalmol*. 2004;25:19–22.
31. Yamamoto N, Itonaga K, Marunouchi T, Majima K. Concentration of transforming growth factor β_2 in aqueous humor. *Ophthalmic Res*. 2005;37:29–33.
32. Ochiai Y, Ochiai H. Higher concentration of transforming growth factor-beta in aqueous humor of glaucomatous eyes and diabetic eyes. *Jpn J Ophthalmol*. 2002;46:249–253.
33. Schlötzer-Schrehardt U, Zenkel M, Küchle M, Sakai LY, Naumann GO. Role of transforming growth factor-β1 and its latent form binding protein in pseudoexfoliation syndrome. *Exp Eye Res*. 2001;73:765–780.
34. Picht G, Welge-Luessen U, Grehn F, Lütjen-Drecoll E. Transforming growth factor β2 levels in the aqueous humor

Investigative Ophthalmology & Visual Science

in different types of glaucoma and the relation to filtering bleb development. *Graefes Arch Clin Exp Ophthalmol*. 2001;239:199–207.
35. Inatani M, Tanihara H, Katsuta H, Honjo M, Kido N, Honda Y. Transforming growth factor-β_2 levels in aqueous humor of glaucomatous eyes. *Graefes Arch Clin Exp Ophthalmol*. 2001;239:109–113.
36. Tripathi RC, Li J, Chan WF, Tripathi BJ. Aqueous humor in glaucomatous eyes contains an increased level of TGF-β2. *Exp Eye Res*. 1994;59:723–727.
37. Harris DL, Joyce NC. Transforming growth factor-beta suppresses proliferation of rabbit corneal endothelial cells in vitro. *J Interferon Cytokine Res*. 1999;19:327–334.
38. Kim TY, Kim WI, Smith RE, Kay ED. Role of $p27^{Kip1}$ in cAMP- and TGF-β2-mediated antiproliferation in rabbit corneal endothelial cells. *Invest Ophthalmol Vis Sci*. 2001;42:3142–3149.
39. Chen KH, Harris DL, Joyce NC. TGF-β2 in aqueous humor suppresses S-phase entry in cultured corneal endothelial cells. *Invest Ophthalmol Vis Sci*. 1999;40:2513–2519.
40. Hori J, Yamaguchi T, Keino H, Hamrah P, Maruyama K. Immune privilege in corneal transplantation. *Prog Retin Eye Res*. 2019;72:100758.
41. Saika S, Liu CY, Azhar M, et al. TGFβ2 in corneal morphogenesis during mouse embryonic development. *Dev Biol*. 2001;240:419–432.
42. Takai Y, Tanito M, Ohira A. Multiplex cytokine analysis of aqueous humor in eyes with primary open-angle glaucoma, exfoliation glaucoma, and cataract. *Invest Ophthalmol Vis Sci*. 2012;53:241–247.
43. Tosi GM, Caldi E, Neri G, et al. HTRA1 and TGF-β1 concentrations in the aqueous humor of patients with neovascular age-related macular degeneration. *Invest Ophthalmol Vis Sci*. 2017;58:162–167.
44. Chang Y, Wu XY. The role of c-Jun N-terminal kinases 1/2 in transforming growth factor β_1-induced expression of connective tissue growth factor and scar formation in the cornea. *J Int Med Res*. 2009;37:727–736.
45. Jester JV, Barry-Lane PA, Cavanagh HD, Petroll WM. Induction of alpha-smooth muscle actin expression and myofibroblast transformation in cultured corneal keratocytes. *Cornea*. 1996;15:505–516.
46. Huh MI, Chang Y, Jung JC. Temporal and spatial distribution of TGF-β isoforms and signaling intermediates in corneal regenerative wound repair. *Histol Histopathol*. 2009;24:1405–1416.
47. Priyadarsini S, McKay TB, Sarker-Nag A, Karamichos D. Keratoconus in vitro and the key players of the TGF-β pathway. *Mol Vis*. 2015;21:577–588.
48. Joyce NC, Harris DL, Mello DM. Mechanisms of mitotic inhibition in corneal endothelium: contact inhibition and TGF-β2. *Invest Ophthalmol Vis Sci*. 2002;43:2152–2159.
49. Ramachandran C, Srinivas SP. Formation and disassembly of adherens and tight junctions in the corneal endothelium: regulation by actomyosin contraction. *Invest Ophthalmol Vis Sci*. 2010;51:2139–2148.
50. Tamura K, Shan WS, Hendrickson WA, Colman DR, Shapiro L. Structure–function analysis of cell adhesion by neural (N-) cadherin. *Neuron*. 1998;20:1153–1163.
51. Itoh F, Itoh S, Adachi T, et al. Smad2/Smad3 in endothelium is indispensable for vascular stability via S1PR1 and N-cadherin expressions. *Blood*. 2012;119:5320–5328.
52. Yang H, Wang L, Zhao J, et al. TGF-β-activated SMAD3/4 complex transcriptionally upregulates N-cadherin expression in non-small cell lung cancer. *Lung Cancer*. 2015;87:249–257.
53. Wecker T, Han H, Borner J, Grehn F, Schlunck G. Effects of TGF-β2 on cadherins and β-catenin in human trabecular meshwork cells. *Invest Ophthalmol Vis Sci*. 2013;54:6456–6462.
54. Yamada S, Nelson WJ. Localized zones of Rho and Rac activities drive initiation and expansion of epithelial cell–cell adhesion. *J Cell Biol*. 2007;178:517–527.
55. Tamura Y, Konomi H, Sawada H, Takashima S, Nakajima A. Tissue distribution of type VIII collagen in human adult and fetal eyes. *Invest Ophthalmol Vis Sci*. 1991;32:2636–2644.
56. Kefalides NA, Cameron JD, Tomichek EA, Yanoff M. Biosynthesis of basement membrane collagen by rabbit corneal endothelium in vitro. *J Biol Chem*. 1976;251:730–733.
57. Jalimarada SS, Ogando DG, Vithana EN, Bonanno JA. Ion transport function of SLC4A11 in corneal endothelium. *Invest Ophthalmol Vis Sci*. 2013;54:4330–4340.
58. Theriault M, Gendron SP, Brunette I, Rochette PJ, Proulx S. Function-related protein expression in Fuchs endothelial corneal dystrophy cells and tissue models. *Am J Pathol*. 2018;188:1703–1712.
59. Ignotz RA, Massague J. Transforming growth factor-β stimulates the expression of fibronectin and collagen and their incorporation into the extracellular matrix. *J Biol Chem*. 1986;261:4337–4345.
60. Maddala R, Reddy VN, Epstein DL, Rao V. Growth factor induced activation of Rho and Rac GTPases and actin cytoskeletal reorganization in human lens epithelial cells. *Mol Vis*. 2003;9:329–336.
61. Wu C, Dedhar S. Integrin-linked kinase (ILK) and its interactors: a new paradigm for the coupling of extracellular matrix to actin cytoskeleton and signaling complexes. *J Cell Biol*. 2001;155:505–510.
62. Rivard N. Phosphatidylinositol 3-kinase: a key regulator in adherens junction formation and function. *Front Biosci (Landmark Ed)*. 2009;14:510–522.
63. Weber GF, Bjerke MA, DeSimone DW. Integrins and cadherins join forces to form adhesive networks. *J Cell Sci*. 2011;124:1183–1193.
64. Okumura N, Kay EP, Nakahara M, Hamuro J, Kinoshita S, Koizumi N. Inhibition of TGF-β signaling enables human corneal endothelial cell expansion in vitro for use in regenerative medicine. *PLoS One*. 2013;8:e58000.
65. Frausto RF, Swamy VS, Peh GSL, et al. Phenotypic and functional characterization of corneal endothelial cells during in vitro expansion. *Sci Rep*. 2020;10:7402.
66. Joyce NC, Harris DL, Zieske JD. Mitotic inhibition of corneal endothelium in neonatal rats. *Invest Ophthalmol Vis Sci*. 1998;39:2572–2583.

Investigative Ophthalmology & Visual Science